# Experimental aspects of heavy flavour production at the LHC

*J. Baines*[a]*, A. Dainese*[b]*, Th. Lagouri*[c]*, A. Morsch*[d]*, R. Ranieri*[e]*, H. Ruiz*[d]*, M. Smizanska*[f]*, and C. Weiser*[g]

[a] Rutherford Laboratory, UK
[b] University and INFN, Padova, Italy
[c] Institute of Nuclear and Particle Physics, Charles University, Prague, Czech Republic
[d] CERN, Geneva, Switzerland
[e] University and INFN, Firenze, Italy
[f] Lancaster University, Lancaster, UK
[g] Institut für Experimentelle Kernphysik, Universität Karlsruhe, Karlsruhe, Germany

**Abstract**

We review selected aspects of the experimental techniques being prepared to study heavy flavour production in the four LHC experiments (ALICE, ATLAS, CMS and LHCb) and we present the expected performance for some of the most significative measurements.

*Coordinators: A. Dainese, M. Smizanska, and C. Weiser*

## 1 Introduction[1]

Unprecedently large cross sections are expected for heavy-flavour production in proton–proton collisions at the LHC energy of $\sqrt{s} = 14$ TeV. Next-to-leading order perturbative QCD calculations predict values of about 10 mb for charm and 0.5 mb for beauty, with a theoretical uncertainty of a factor 2–3. Despite these large cross sections, the LHC experiments, ALICE [1,2], ATLAS [3], CMS [4], and LHCb [5], will have to deal with rejection of background coming from non-heavy flavour inelastic interactions for which the predicted cross is about 70 mb. The four experiments will work at different luminosity conditions. ATLAS and CMS are designed to work in a wide range of luminosities up to nominal $10^{34}$ cm$^{-2}$s$^{-1}$, while the LHCb optimal luminosity will vary in the range $(2\text{–}5) \times 10^{32}$ cm$^{-2}$s$^{-1}$ and ALICE is designed to work at $3 \times 10^{30}$ cm$^{-2}$s$^{-1}$ in proton–proton collisions. Luminosity conditions in ATLAS, CMS and LHCb allow multiple interactions per bunch crossing, thus leading to requirements of even stronger identification and selection of heavy-flavour events already at trigger level. The first task will be the measurement of integrated and differential charm and beauty production cross sections in the new energy domain covered at the LHC. ALICE will play an important role, having acceptance down to very low transverse momentum, as we discuss in Section 4. These measurements can be performed within a relatively short period of running. Afterwards, the heavy-flavour studies will focus on less inclusive measurements addressing specific production mechanisms that allow to test higher order perturbative QCD predictions, as well as on rare decays of heavy-flavour hadrons, that may carry information on New Physics beyond the Standard Model. In order to meet these requirements dedicated and sophisticated trigger strategies have been prepared by the LHC experiments.

## 2 Heavy flavour detection in the LHC experiments[2]

The four detectors that will take data at the LHC have different features and design requirements, but all of them are expected to have excellent capabilities for heavy-flavour measurements. Their complementarity will provide a very broad coverage in terms of phase-space, decay channels and observables.

[1] Author: M. Smizanska
[2] Author: A. Dainese

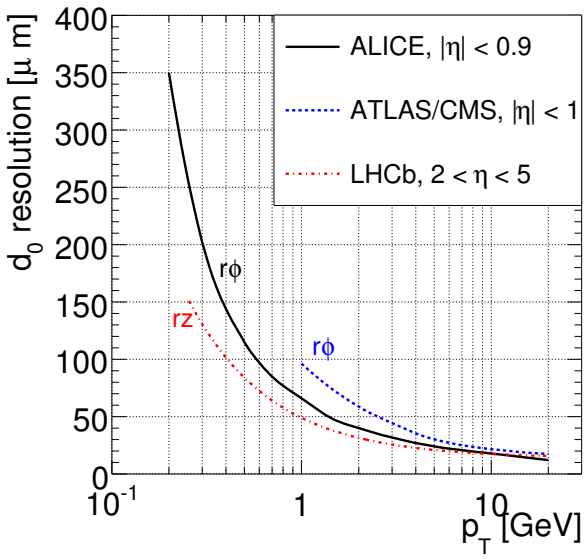


**Fig. 1:** Track impact parameter resolutions for the four LHC experiments. Note that for ALICE, ATLAS and CMS the impact parameter is defined in the $r\phi$ plane, while for LHCb it is defined in the $rz$ plane.

Experimentally, the key elements for a rich heavy-flavour program are track and vertex reconstruction and particle identification (PID).

Open charm and beauty mesons have typical life-times in the order of a $ps$ ($c\tau$ values are about 125–300 $\mu$m for D mesons and 500 $\mu$m for B mesons) and the most direct detection strategy is the identification of single tracks or vertices that are displaced from the interaction vertex. The detector capability to perform this task can be characterized by the transverse impact parameter[3] ($d_0$) resolution. All experiments will be equipped with high position-resolution silicon-detector layers, including pixel detector for the innermost layers, for precise tracking and impact parameter measurement. Tracking is done in the central (pseudo)rapidity region for ALICE ($|\eta| < 0.9$), ATLAS and CMS ($|\eta| \lesssim 2.5$), and in the forward region for LHCb ($2 \lesssim \eta \lesssim 5$). In Fig. 1 we show the $d_0$ resolution, which is similar for the different experiments, and better than 50 $\mu$m for $p_T \gtrsim 1.5$–3 GeV. The inner detector systems of ATLAS, CMS and ALICE will operate in different magnetic fields: The ALICE magnetic field will vary within low values (0.2–0.5 T) leading to a very low $p_T$ cutoff of 0.1–0.2 GeV, while ATLAS (2 T) and CMS (4 T) have higher cutoffs of 0.5 and 1 GeV, respectively, but better $p_T$ resolution at high $p_T$ (e.g., at $p_T = 100$ GeV, $\delta p_T/p_T \approx 1$–$2\%$ for ATLAS/CMS at central rapidity and $\approx 9\%$ for ALICE).

Both lepton and hadron identification are important for heavy-flavour detection. D and B mesons have relatively large branching ratios (BR) in the semi-leptonic channels, $\simeq 10\%$ to electrons and $\simeq 10\%$ to muons, and inclusive cross-section measurements can be performed via single leptons or di-leptons. Alternatively, high-$p_T$ leptons can be used as trigger-level tags to select $\mathrm{B} \rightarrow \mathrm{J}/\psi + X$ candidate events, that provide more accurate cross section measurements. ALICE can identify electrons with $p_T > 1$ GeV and $|\eta| < 0.9$, via transition radiation and $\mathrm{d}E/\mathrm{d}x$ measurements, and muons in the forward region, $2.5 < \eta < 4$, which allows a very low $p_T$ cutoff of 1 GeV. CMS and ATLAS have a broad pseudorapidity coverage for muons, $|\eta| < 2.4$ and $|\eta| < 2.7$, respectively, but they have a higher $p_T$ cutoff varying between 4 and 6 GeV, depending on $\eta$. Both CMS and ATLAS have high-resolution electro-magnetic calorimeters that will be used to identify electrons. Semi-leptonic inclusive measurements do not provide direct information on the D(B)-meson $p_T$ distribution, especially at low $p_T$, because of the weak corre-

[3] We define as impact parameter the distance of closest approach to the interaction vertex of the track projection in the plane transverse to the beam direction.

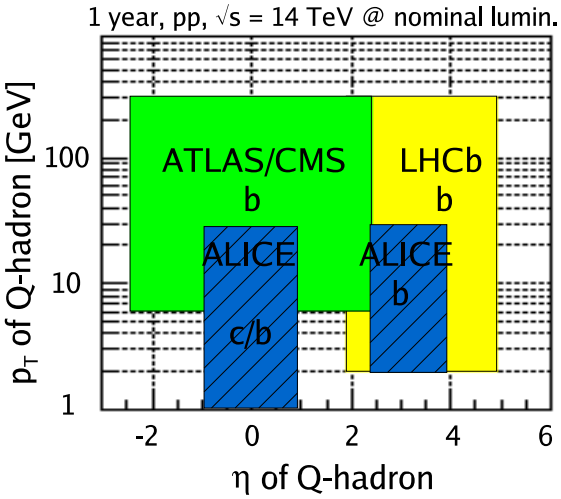


**Fig. 2:** Schematic acceptances in transverse momentum and pseudorapidity for open heavy flavour hadrons (indicated as 'Q-hadrons') in the four LHC experiments. The high-$p_T$ coverages correspond to one year (i.e. 7 months) of running at nominal luminosity (see beginning of this section).

lation between the lepton and the meson momenta. Therefore, for charm in particular, the reconstruction of exclusive (hadronic) decays is preferable. In this case, hadron identification allows a more effective rejection of the combinatorial background in the low-$p_T$ region. ALICE disposes of $\pi/\mathrm{K}/\mathrm{p}$ separation via $\mathrm{d}E/\mathrm{d}x$ and time-of-flight measurements for $p < 3$–$4$ GeV and $|\eta| < 0.9$.

Figure 2 shows schematically the $p_T$ vs. $\eta$ acceptances for charm (c) and beauty (b) hadrons in the four experiments, as expected for one year of running at nominal luminosity (note that the value of the luminosity is different for each experiment, as previously discussed). ATLAS and CMS have similar acceptances for beauty measurements; the minimum accessible $p_T$ is relatively large because of the strong magnetic fields, which in turn, together with the high luminosity, allow to cover transverse momenta up to 200–300 GeV. The acceptance of LHCb, although centred at forward rapidity, has a significant overlap, with those of ATLAS and CMS. The acceptance of ALICE for beauty overlaps with ATLAS and CMS at central rapidity and with LHCb at forward rapidity. The moderate magnetic field allows measurements down to transverse momenta of about 2 GeV for B mesons in the forward muon arm and in the barrel, and down to about 1 GeV for D mesons in the barrel.

## 3 Beauty triggers at the LHC

### 3.1 ATLAS beauty trigger[4]

The ATLAS trigger consists of three levels [6]. Level-1 is implemented in hardware, whilst the higher level triggers (level-2 and the Event Filter, EF) are based on general-purpose processors. The level-1 triggers are based on information from the calorimeter and muon trigger chambers. At higher trigger levels, information from the Inner Detector (ID) and precision muon detector is included. The size of the level-2 and EF processor farms is limited, which in turn limits the amount of data processing that can be performed in the trigger. The B-trigger must, therefore, have the flexibility to adapt selections both as the luminosity falls during a beam-coast and, over a longer time-scale, as the peak luminosity of the LHC increases. This is achieved by using a di-muon trigger at the start of higher luminosity fills and introducing additional triggers for lower luminosity fills or as the luminosity falls during a beam coast [7].

[4]Author: J. Baines

A di-muon trigger provides a very effective selection for a range of important channels, e.g. $\mathrm{B_d^0} \to \mathrm{J}/\psi(\mu^+\mu^-)\mathrm{K_s^0}$, $\mathrm{B} \to \mathrm{K}^{0\star}\mu\mu$ and $\mathrm{B} \to \rho^0\mu\mu$. The Level-1 muon trigger is efficient down to a $p_T$ of about 5 GeV in the barrel region and about 3 GeV in the end-caps. However the actual thresholds used for the di-muon trigger will be determined by rate limitations. For example, a $p_T$ threshold of 6 GeV would give a di-muon trigger rate of about 600 Hz after level-1 at a luminosity of $2 \times 10^{33}$ cm$^{-2}$s$^{-1}$. These triggers are mostly due to muons from heavy flavour decays plus some single muons which are doubly counted due to overlaps in the end-cap trigger chambers. The later are removed when the muons are confirmed at level-2 using muon precision chambers and ID information from inside the level-1 Region of Interest (RoI). At the EF tracks are refit, inside regions identified by level-2, and specific selections made on the basis of mass and decay length cuts. These consist of semi-inclusive selections, for example to select $\mathrm{J}/\psi(\mu^+\mu^-)$ decays with a displaced vertex, and in some cases exclusive selections such as for $\mathrm{B} \to \mu^+\mu^-$. The final trigger rate, after the EF, is about 20 Hz at a luminosity of $2 \times 10^{33}$ cm$^{-2}$s$^{-1}$.

At lower luminosities, additional triggers are introduced which are based on a single muon trigger ($p_T \gtrsim 8$ GeV) together with a calorimeter trigger. The calorimeter trigger identifies clusters of energy deposition in the electromagnetic and hadronic calorimeter consistent with an electron or photon (EM RoI) or a jet (Jet RoI). For hadronic final states, such as $\mathrm{B_s^0} \to \mathrm{D_s^-}\pi^+$ and $\mathrm{B_s^0} \to \mathrm{D_s^-a_1^+}$ track are reconstructed in the Inner Detector in RoI of about $\Delta\eta \times \Delta\phi = 1.0 \times 1.5$. By limiting track reconstruction to the part of the ID lying within the RoI, about 10% on average, there is potential for up to a factor of ten saving in execution time compared to reconstruction in the full Inner Detector. Preliminary studies of efficiency and jet-cluster multiplicity have been made using a fast simulation which includes a detailed parameterization of the calorimeter. These studies indicate that a threshold on the jet cluster energy of $E_T > 5$ GeV gives a reasonable multiplicity, i.e. a mean of about two RoI per event for events containing a muon trigger. This threshold would give a trigger that is efficient for $\mathrm{B_s^0} \to \mathrm{D_s^-}\pi^+$ events with a $B$-hadron $p_T$ above about 15 GeV.

Track reconstruction inside e/gamma RoI can be used to select channels such as $\mathrm{B_d} \to \mathrm{K}^{0\star}\gamma$, $\mathrm{B_d^0} \to \mathrm{J}/\psi(e^+e^-)\mathrm{K_s^0}$, and $\mathrm{B_s} \to \phi\gamma$. Preliminary studies show that a reasonable compromise between RoI multiplicity and electron efficiency might be obtained with a cluster energy threshold of $E_T > 2$ GeV. This gives a mean RoI multiplicity of about one for events containing a muon trigger and is efficient for channels containing an electron with $p_T > 5$ GeV. Following the ID track reconstruction further selections are made for specific channels of interest. These are kept as inclusive as possible at level-2 with some more exclusive selections at the EF.

In LHC running, there will be competing demands for resources in the level-2 and EF trigger farms and for trigger band-width. By adopting a flexible strategy and making the maximum use of RoI information to guide reconstruction at level-2 and the EF, the B-physics coverage of ATLAS can be maximized.

### 3.2 CMS beauty trigger[5]

The Large Hadron Collider (LHC) will provide 40 MHz proton-proton collisions at the centre of mass energy of 14 TeV. At the beginning a luminosity of $2\times10^{33}$ cm$^{-2}$s$^{-1}$ is expected, corresponding to 20 fb$^{-1}$ collected per year. Assuming the $\mathrm{b\overline{b}}$ production cross section to be 0.5 mb, $10^{13}$ b-physics events per year are foreseen: all kind of b-particles will be produced and studies will be performed not only in $\mathrm{B_d^0}$, but also in $\mathrm{B_s^0}$ meson system. A wide b-physics programme, including CP violation, $\mathrm{B_s^0} - \overline{\mathrm{B}}_\mathrm{s}^0$ mixing and rare decays can therefore be covered by the CMS experiment. The apparatus will be equipped with a very precise tracking system made with silicon microstrip and pixel detectors [8, 9].

The rate at which events can be archived for offline analyses is 100 Hz [10, 11]. The trigger thresholds are optimized for a wide physics discovery program with selection of high transverse momentum

[5] Author: R. Ranieri

($p_T$) processes. Low-$p_T$ events, as required for b-physics , are selected mainly by the first level muon trigger, then an exclusive reconstruction of few relevant *benchmark* channels can separate interesting events from the background. The b-physics programme could evolve with time following both the theoretical developments and the results which will be obtained in the next years by b-factories and Tevatron experiments.

The lowest trigger level (Level-1) is based on the fast response of calorimeters and muon stations with coarse granularity. No information on secondary vertices is available, hence the Level-1 selection of b-physics events exploits the leptonic signatures from beauty hadron decays, therefore a single muon or a di-muon pair is required. The Level-1 output at start-up will be 50 kHz. Several studies have been done to optimize the trigger thresholds in order to have the possibility of selecting most of the interesting physics signatures. A total of 3.6 kHz rate is dedicated to the Level-1 muon selection. It is obtained by requiring a single muon with $p_T > 14$ GeV or at least two muons with $p_T > 3$ GeV.

A further selection is made during the High-Level trigger (HLT) by using also the information from the tracking system. The CMS High-Level trigger is entirely based on a CPU farm with some thousand CPUs. Each processor analyses a single event; in principle offline event reconstruction can be performed, but in order to reduce the processing time fast track reconstruction has to be done. Some algorithms will be dedicated to the fast reconstruction and identification of physics processes, thus allowing to start the offline analysis directly from the online selection. They have to fulfill the HLT time constraint, hence they have to be able to analyze and accept (or reject) data within the time limits imposed by the HLT latency. To lower the execution time, which is due mainly to the processing of tracking system signals, track reconstruction is preferably performed only in limited regions of the space (*regional track reconstruction*) and stopped when a certain precision is reached in the measurement of some track parameters, such as transverse momentum and impact parameter (*conditional track finding*). Invariant mass of b-hadrons can thus be measured online with good resolution, allowing to select the searched event topologies.

An additional trigger strategy, which relies on the possibility of lowering the trigger thresholds during the LHC beam coast or lower luminosity fills to collect more b-physics events is under study.

The rare decay $\mathrm{B}^0_{\mathrm{s,d}} \to \mu^+\mu^-$ is triggered at Level-1 with 15.2% efficiency. At HLT, the two muons are required to be opposite charged and isolated, to come from a displaced common vertex and have an invariant mass within 150 MeV from the $\mathrm{B}^0_{\mathrm{s}}$ mass. The estimated background rate is below 2 Hz and nearly 50 signal events are expected with 10 fb$^{-1}$.

The determination of $\Delta m_s$ and $\Delta\Gamma_s$ will be a valuable input for flavour dynamics in the Standard Model and its possible extensions. The measurement of $\Delta m_s$ is allowed by the $\mathrm{B}^0_{\mathrm{s}} \to \mathrm{D_s}^-\pi^+$ decay followed by $\mathrm{D_s}^- \to \phi\pi^-$ and $\phi \to \mathrm{K}^+\mathrm{K}^-$. The $\mathrm{B}^0_{\mathrm{s}}$ CP state at decay time is tagged by the charge of the pion associated to the $\mathrm{D_s}$ (in this case the $\pi^+$). The only way to trigger on these hadronic events is to search for the muon coming from the decay of the other b quark in the event. In addition to the single muon Level-1 trigger, it was studied the possibility of a combined trigger with a low-$p_T$ muon and a soft jet. The CMS High-Level trigger algorithm reconstructs the charged particle tracks with only three points by using the precise pixel detector. Topological and kinematical cuts are applied to reconstruct the three resonances $\phi$, $\mathrm{D_s}$ and $\mathrm{B}^0_{\mathrm{s}}$. A 20 Hz output rate is achieved with about 1000 signal events in 20 fb$^{-1}$. Since the overall possible rate on tape is 100 Hz, the bandwidth allocated to this channel probably could not exceed 5 Hz. If the fraction of events written to tape is scaled accordingly, more than 300 signal events are expected for 20 fb$^{-1}$. In order to fully cover the range allowed by the Standard Model, about 1000 events are needed.

The decay channel $\mathrm{B}^0_{\mathrm{s}} \to \mathrm{J}/\psi\phi$ is very important because it can not be studied with large accuracy before LHC and can reveal hints for physics beyond the Standard Model. Events with a couple of muons are passed to the HLT. The inclusive selection of $\mathrm{J}/\psi \to \mu^+\mu^-$ decays, obtained with mass requirements on the di-muon system, leads to a total of 15 Hz rate, 90% of which is made of $\mathrm{J}/\psi$ from b quarks. With an additional amount of CPU time, perhaps sustainable by the HLT computing power, about 170 000 events are expected in 20 fb$^{-1}$ with less than 2 Hz rate.

### 3.3 LHCb beauty trigger[6]

The LHCb detector [5] is optimized for exploiting the B-physics potential of LHC. Together with excellent vertexing and particle identification, an efficient trigger on a wide variety of B decays is one of the main design requirements of the experiment.

The LHCb trigger system [12] is organized in three levels. The first one (L0) runs on custom electronics and operates synchronously at 40 MHz, with a 4 $\mu$s latency. The remaining two trigger levels (L1 and HLT) run on a shared farm of 1400 commercial CPUs. A brief description of the three trigger levels and their performance follows.

L0 exploits the relatively high $p_T$ of B decay products. High $p_T$ candidates are identified both in the calorimeter and in the muon system, with $p_T$ thresholds of about 3 and 1 GeV respectively. Complicated events that would consume unreasonable time at higher levels are promptly vetoed in two different ways. First, multiple primary vertex topologies are rejected by using two dedicated silicon layers of the vertex detector. Secondly, events with large multiplicity, measured at a scintillating pad layer, are vetoed. The input rate of events visible in the detector is about 10 MHz, with a $b\overline{b}$ content of 1.5%. L0 reduces this rate by a factor of 10 while increasing the $b\overline{b}$ content to 3%. The typical efficiency of L0 is 90% for channels with dimuons, 70% for radiative decays and 50% for purely hadronic decays.

At the 1 MHz input rate of L1 it becomes feasible to use tracking information, allowing for the search for B vertex displacement signatures. Tracks are first searched at the vertex detector, and then confirmed in two dedicated tracking layers (trigger tracker or TT) which provide a rough estimation of the momentum of the tracks ($\delta p_T/p_T \sim 25\%$). The generic L1 decision is based on the presence of two tracks with an impact parameter higher than 0.15 mm with a sufficiently high value of $log(p_{T1} + p_{T2})$. Alternative selection criteria are applied, based on the presence of tracks matched to L0 neutral calorimeter objects and muon candidates. The output rate of L1 is 40 kHz with a $b\overline{b}$ content of 15%. The efficiencies are at the level of 90, 80 and 70% for channels with di-muons, only hadrons and radiative decays respectively.

The HLT [13] consists of two sequential *layers*. The first one refines the L1 decision with the all the tracking information from the detector, improving the $p_T$ measurement to the level of $\delta p_T/p_T \sim 1\%$. The rate is reduced to 13 kHz and the $b\overline{b}$ content is enriched to 30%. The second layer consists on a series of alternative selections. A first group of them aims for maximal efficiency on the base-line physics channels and the corresponding control samples, by making use of the complete reconstruction of the decay vertex and its kinematical properties. These selections fill 200 Hz of bandwidth, while providing efficiencies typically higher than 90%. The rest of selections aim for more generic signatures that will provide robustness and flexibility to the trigger system. In addition, the samples selected will be useful for calibration and systematic studies. The selections aim for generic J/$\psi$ and D$^\star$ (600 Hz and 300 Hz respectively), and generic B decays (900 Hz). The latter is based on the detection of single muons with high $p_T$ and impact parameter.

In total, 2 kHz of events will be written on tape, with an expected overall efficiency ranging between 75% for channels with di-muons to 35% for purely hadronic final states.

## 4 Measurements in preparation at the LHC and expected performance

In the following we present, as examples, the expected performance for the detection of D and B mesons in ALICE[7], and for the study of $\mathrm{b\overline{b}}$ azimuthal correlation in ATLAS. We also include a summary of the capability of ALICE of quarkonia measurements ($\psi$ family and $\Upsilon$ family).

[6] Author: H. Ruiz

[7] Given that ALICE is dedicated to the study of nucleus–nucleus collisions at the LHC, some of the presented results are relative to Pb–Pb collisions at $\sqrt{s} = 5.5$ TeV per nucleon–nucleon collisions. These results can be taken as lower limits for the performance in pp collisions, where the background contributions are much lower.

### 4.1 Charm reconstruction in ALICE[8]

One of the most promising channels for open charm detection is the $\mathrm{D}^0 \rightarrow \mathrm{K}^-\pi^+$ decay (and charge conjugate) that has a BR of 3.8%. The expected yields ($\mathrm{BR} \times \mathrm{d}N/\mathrm{d}y$ at $y = 0$), in pp collisions at $\sqrt{s} = 14$ TeV and in central Pb–Pb (0–5% $\sigma^{\mathrm{tot}}$) at $\sqrt{s_{\mathrm{NN}}} = 5.5$ TeV are $7.5 \times 10^{-4}$ and $5.3 \times 10^{-1}$ per event, respectively [14].

The main feature of this decay topology is the presence of two tracks with impact parameters $d_0 \sim 100\ \mu\mathrm{m}$. The detection strategy [15] to cope with the large combinatorial background from the underlying event is based on the selection of displaced-vertex topologies, i.e. two tracks with large impact parameters and good alignment between the $\mathrm{D}^0$ momentum and flight-line, and on invariant-mass analysis to extract the signal yield. This strategy was optimized separately for pp and Pb–Pb collisions, as a function of the $\mathrm{D}^0$ transverse momentum, and statistical and systematic errors were estimated [16, 17]. The results, in terms of $p_T$ coverage and statistical precision, are found to be similar for the two colliding systems [16, 17].

Figure 3 (left) shows the expected sensitivity of ALICE for the measurement of the $\mathrm{D}^0$ $p_T$-differential cross section in pp collisions, along with NLO pQCD [18] calculation results corresponding to different choices of the charm quark mass and of renormalization and factorization scales. In the right-hand panel of the figure we present the ratio 'data/theory' ('default parameters/theory parameters') which better allows to compare the different $p_T$-shapes obtained by changing the input 'theory parameters' and to illustrate the expected sensitivity of the ALICE measurement. The estimated experimental errors are much smaller than the theoretical uncertainty band. We note that the data cover the region at low transverse momentum where the accuracy of the pQCD calculation becomes poorer and where novel effects, determined by the high partonic density of the initial state at LHC energies, may play an important role (see "Small-$x$ effects in heavy quark production" section of this report).

### 4.2 Beauty production measurements in ALICE[9]

The expected yields ($\mathrm{BR} \times \mathrm{d}N/\mathrm{d}y$ at $y = 0$) for $\mathrm{B} \rightarrow e^{\pm} + X$ plus $\mathrm{B} \rightarrow \mathrm{D}\,(\rightarrow e^{\pm} + X) + X'$ in pp collisions at $\sqrt{s} = 14$ TeV and in central Pb–Pb (0–5% $\sigma^{\mathrm{tot}}$) at $\sqrt{s_{\mathrm{NN}}} = 5.5$ TeV are $2.8 \times 10^{-4}$ and $1.8 \times 10^{-1}$ per event, respectively [14].

The main sources of background electrons are: (a) decays of D mesons; (b) neutral pion Dalitz decays $\pi^0 \rightarrow \gamma e^+ e^-$ and decays of light mesons (e.g. $\rho$ and $\omega$); (c) conversions of photons in the beam pipe or in the inner detector layers and (d) pions misidentified as electrons. Given that electrons from beauty have average impact parameter $d_0 \simeq 500\ \mu\mathrm{m}$ and a hard momentum spectrum, it is possible to obtain a high-purity sample with a strategy that relies on: electron identification with a combined $\mathrm{d}E/\mathrm{d}x$ and transition radiation selection, which allows to reduce the pion contamination by a factor $10^4$; impact parameter cut to reject misidentified pions and electrons from sources (b) and (c); transverse momentum cut to reject electrons from charm decays. As an example, with $d_0 > 200\ \mu\mathrm{m}$ and $p_T > 2$ GeV, the expected statistics of electrons from B decays is $8 \times 10^4$ for $10^7$ central Pb–Pb events, allowing the measurement of electron-level $p_T$-differential cross section in the range $2 < p_T < 18$ GeV. The residual contamination of about 10%, acculated in the low-$p_T$ region, of electrons from prompt charm decays and from misidentified charged pions can be evaluated and subtracted using a Monte Carlo simulation tuned to reproduce the measured cross sections for pions and $\mathrm{D}^0$ mesons. A Monte-Carlo-based procedure can then be used to compute, from the electron-level cross section, the B-level cross section $\mathrm{d}\sigma^{\mathrm{B}}(p_T > p_T^{\mathrm{min}})/\mathrm{d}y$ [17]. In the left-hand panel of Fig. 4 we show this cross section for central Pb–Pb collisions with the estimated uncertainties. The covered range is $2 < p_T^{\mathrm{min}} < 30$ GeV.

B production can be measured also in the ALICE forward muon spectrometer, $2.5 < \eta < 4$, analyzing the single-muon $p_T$ distribution and the opposite-sign di-muons invariant mass distribution [17].

[8] Author: A. Dainese

[9] Author: A. Dainese

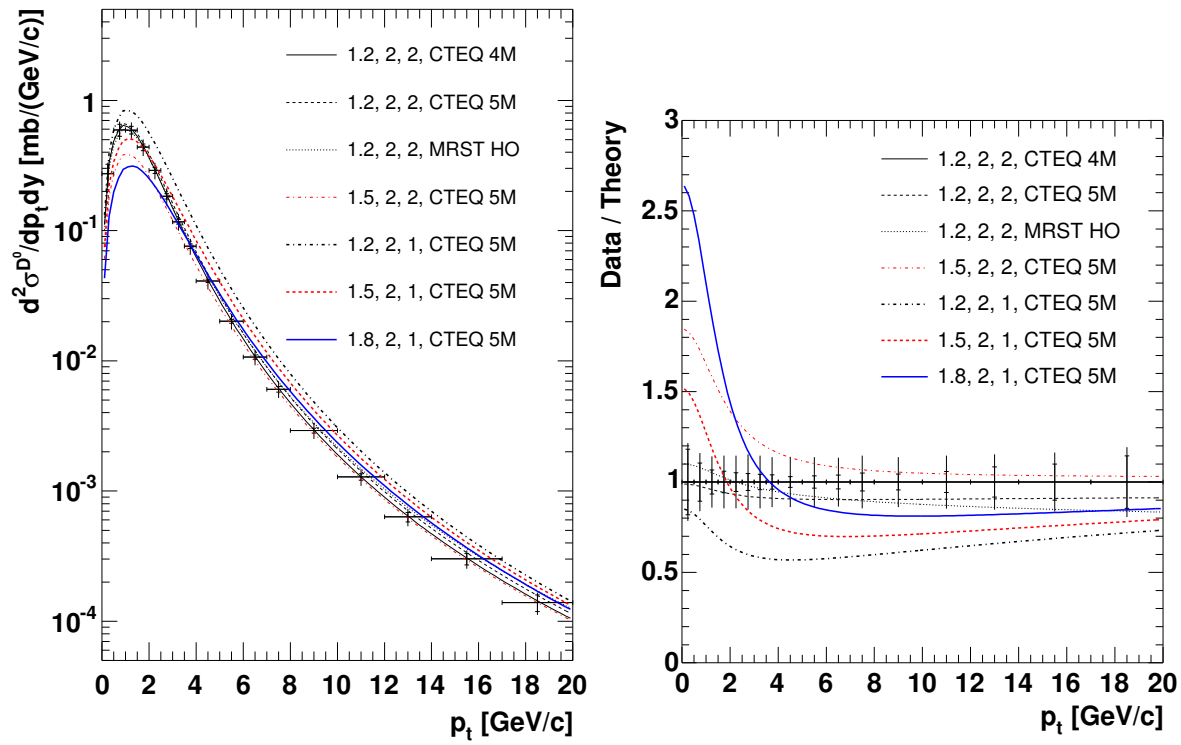


**Fig. 3:** ALICE sensitivity on $\mathrm{d}^2\sigma^{\mathrm{D}^0}/\mathrm{d}p_T\mathrm{d}y$, in pp at 14 TeV, compared to the pQCD predictions obtained with different sets of the input parameters $m_c$ [GeV], $\mu_F/\mu_0$, $\mu_R/\mu_0$ and PDF set ($\mu_0$ is defined in the text). The inner bars represent the statistical error, the outer bars the quadratic sum of statistical and $p_T$-dependent systematic errors. A normalization error of 5% is not shown. The panel on the right shows the corresponding 'data/theory' plot.

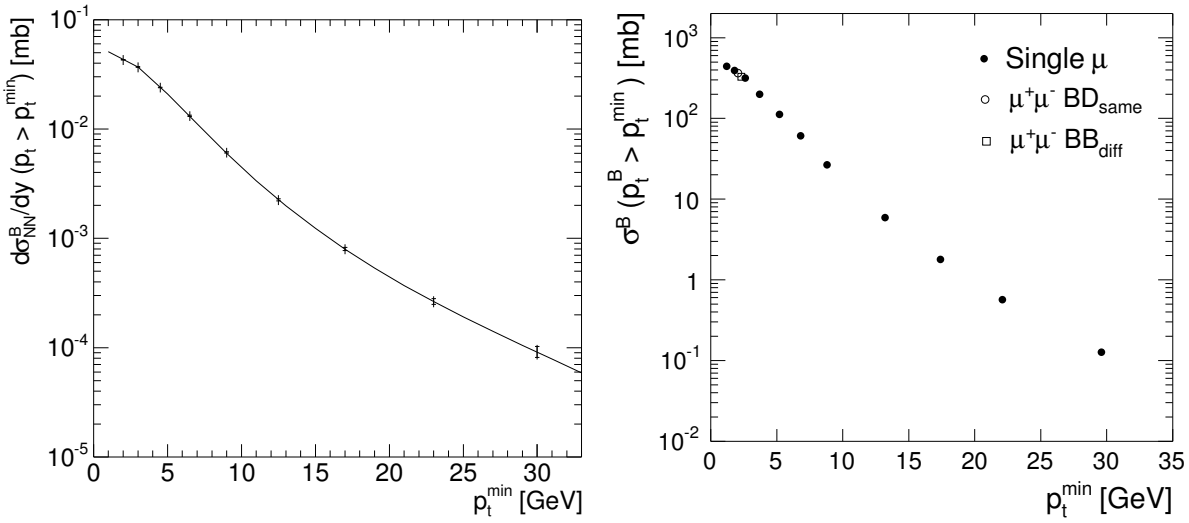


**Fig. 4:** B production cross section vs. $p_T^{\mathrm{min}}$ reconstructed by ALICE in $10^7$ central Pb–Pb events. Left: $\mathrm{d}\sigma^{\mathrm{B}}_{\mathrm{NN}}/\mathrm{d}y$ at $y = 0$ (normalized to one nucleon–nucleon collision) from single electrons in $|\eta| < 0.9$; statistical (inner bars) and quadratic sum of statistical and $p_T$-dependent systematic errors (outer bars) are shown; a 9% normalization error is not shown. Right: $\sigma^{\mathrm{B}}$ integrated in $2.5 < y^{\mathrm{B}} < 4$ (not normalized to one nucleon–nucleon collision) from single muons and di-muons in $2.5 < \eta < 4$; only (very small) statistical errors shown.

The main backgrounds to the 'beauty muon' signal are $\pi^{\pm}$, $\mathrm{K}^{\pm}$ and charm decays. The cut $p_T > 1.5$ GeV is applied to all reconstructed muons in order to increase the signal-to-background ratio. For the opposite-sign di-muons, the residual combinatorial background is subtracted using the technique of event-mixing and the resulting distribution is subdivided into two samples: the low-mass region, $M_{\mu^+\mu^-} < 5$ GeV, dominated by muons originating from a single b quark decay through $\mathrm{b} \rightarrow \mathrm{c}(\rightarrow \mu^+)\mu^-$ ($\mathrm{BD}_{\mathrm{same}}$), and the high-mass region, $5 < M_{\mu^+\mu^-} < 20$ GeV, dominated by $\mathrm{b\overline{b}} \rightarrow \mu^+\mu^-$, with each muon coming from a different quark in the pair ($\mathrm{BB}_{\mathrm{diff}}$). Both samples have a background from $\mathrm{c\overline{c}} \rightarrow \mu^+\mu^-$ and a fit is done to extract the charm- and beauty-component yields. The single-muon $p_T$ distribution has three components with different slopes: K and $\pi$, charm, and beauty decays. Also in this case a fit technique allows to extract a $p_T$ distribution of muons from B decays. A Monte Carlo procedure, similar to that used for semi-electronic decays, allows to extract B-level cross sections for the data sets (low-mass $\mu^+\mu^-$, high-mass $\mu^+\mu^-$, and $p_T$-binned single-muon distribution), each set covering a specific B-meson $p_T > p_T^{\mathrm{min}}$ region, as preliminarly shown in Fig. 4 (right). Since only minimal cuts are applied, the reported statistical errors are very small and high-$p_T$ reach is excellent. Systematic errors are currently under study.

### 4.3 Study of $\mathrm{b\overline{b}}$ correlations in ATLAS[10]

The ATLAS detector [19] is well engineered for studies of b-production, and together with the huge rate of b-quark production that will be seen at LHC, offers great potential for the making of novel precise b production measurements. Correlations between b and $\overline{\mathrm{b}}$ quarks and events with more than one heavy-quark pair, $\mathrm{b\overline{b}b\overline{b}}$, $\mathrm{b\overline{b}c\overline{c}}$, $\mathrm{b\overline{b}s\overline{s}}$, that were difficult to access in previous experiments due to limited statistics, will be investigated in detail. A new technique has been developed in ATLAS for measuring correlations, and this will yield results that will shed new light on our understanding of the QCD cross-section for $\mathrm{b\overline{b}}$-production.

A detailed study investigated a possibility of $\mathrm{b\overline{b}}$ correlations measurement using the $\Delta\phi$(J/$\psi$-$\mu$) distribution, the azimuthal separation of a J/$\psi$ and a muon [20–22]. This technique is expected to be superior to earlier methods used at the Tevatron Run-1 based on muon–muon or muon–b-jet correlations. The new method does not require separation cuts between the two objects. Such cuts were necessary to control the background, but they required a model-dependent extrapolation of the results to full azimuthal space [23]. Using a full simulation of the Inner Detector and the Muon Spectrometer of the ATLAS detector [19] it is shown that such a distribution can be extracted from heavy flavour events at LHC.

ATLAS studies were done for two channels selected to measure the azimuthal angle difference $\Delta\phi(\mathrm{b\overline{b}})$ between b and $\overline{\mathrm{b}}$ quarks:

$$\overline{\mathrm{b}} \rightarrow \mathrm{B_d} \rightarrow \mathrm{J}/\psi(\rightarrow \mu\mu)\mathrm{K}^0\,, \quad \mathrm{b} \rightarrow \mu + \mathrm{X} \quad \text{and} \quad \overline{\mathrm{b}} \rightarrow \mathrm{B_s} \rightarrow \mathrm{J}/\psi(\rightarrow \mu\mu)\phi\,, \quad \mathrm{b} \rightarrow \mu + \mathrm{X}\,.$$

The numbers of events expected for 30 fb$^{-1}$ as might be achieved after 3 years of running at a luminosity of $10^{33}$ cm$^2$s$^{-1}$ are $4.8\times10^4$ and $3.2\times10^4$ respectively for these channels. No isolation cuts are needed to separate exclusively reconstructed B-decays from the muon produced in the semi-leptonic decay of the other B-particle in the event. The reconstruction efficiency remains high in topologies where the azimuthal angle difference $\Delta\phi$(J/$\psi$-$\mu$) between J/$\psi$ and the muon is small.

Special attention was devoted to background events in which the muon is produced from the decays $\mathrm{K}^{\pm}$, $\pi^{\pm} \rightarrow \mu^{\pm} + X$ instead of b$\rightarrow \mu + X$. The study showed that this background is not problematic in $\mathrm{B_d}$ decays, however it is important in the case of $\mathrm{B_s^0}$ meson.

In summary, the results of the analysis suggest that backgrounds from K/$\pi$ decays are small, and that backgrounds from events containing 4 b quarks are relatively flat in $\Delta\phi$(J/$\psi$-$\mu$). The efficiency of the reconstruction of muons with this technique is also relatively flat in $\Delta\phi$(J/$\psi$-$\mu$) and so we conclude that corrections to the measured $\Delta\phi$(J/$\psi$-$\mu$) distribution are likely to be small.

[10] Author: Th. Lagouri

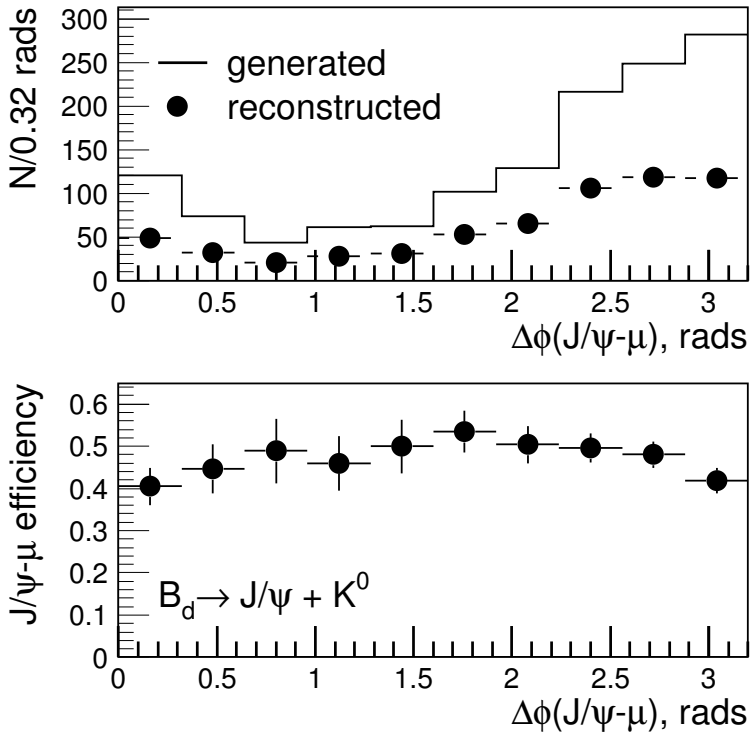


**Fig. 5:** Distribution of the opening angle $\Delta\phi$(J/$\psi$-$\mu$) between the J/$\psi$ from the decay $\mathrm{B_d} \rightarrow \mathrm{J}/\psi\mathrm{K}^0$ and the muon coming from the associated B hadron decay to muon, both direct $\mathrm{b} \rightarrow \mu$ and indirect $\mathrm{b} \rightarrow \mathrm{c} \rightarrow \mu$.

### 4.4 Quarkonia measurements in ALICE[11]

Heavy quarkonia states are hard, penetrating probes which provide an essential tool to study the earliest and hottest stages of heavy-ion collisions [24]. They can probe the strongly interacting matter created in these reactions on short distance scales and are expected to be sensitive to the nature of the medium, i.e. confined or de-confined [25, 26]. The suppression (dissociation) of the heavy-quark resonances is considered as one of the most important observables for the study of the QGP at the LHC (see Ref. [2] for a recent review).

In ALICE, quarkonia will be measured in the di-electron channel using a barrel ($|\eta| < 0.9$) Transition Radiation Detector (TRD) [2] and in the di-muon channel using a forward Muon Spectrometer ($2.5 < \eta < 4$) [2]. The complete spectrum of heavy-quark vector mesons (J/$\psi$, $\psi'$, $\Upsilon$, $\Upsilon'$, $\Upsilon''$) can be measured down to zero $p_T$. In particular the good mass resolution allows to resolve the Upsilon family.

The Muon Spectrometer uses a low-$p_T$ trigger threshold, $p_T > 1$ GeV, on single muons for charmonia and a high-$p_T$ trigger, $p_T > 2$ GeV, for bottonia detection. The TRD can trigger on single electrons with $p_T > 3$ GeV, which results in a minimum transverse momentum of triggered charmonia of $5.2$ GeV. Electron identification combined with the excellent vertexing capabilities of the inner tracking system allows ALICE to distinguish direct charmonium production from secondary charmonium production through B decays.

The energy density dependence will be studied by varying the impact parameters and by studying in addition to the heaviest collision system (Pb–Pb) also intermediate mass and low mass A–A systems. To determine the primary production cross-section of the resonances and the amount of pre-resonance absorption, corresponding measurement have to be performed for pA and pp collisions.

[11] Author: A. Morsch

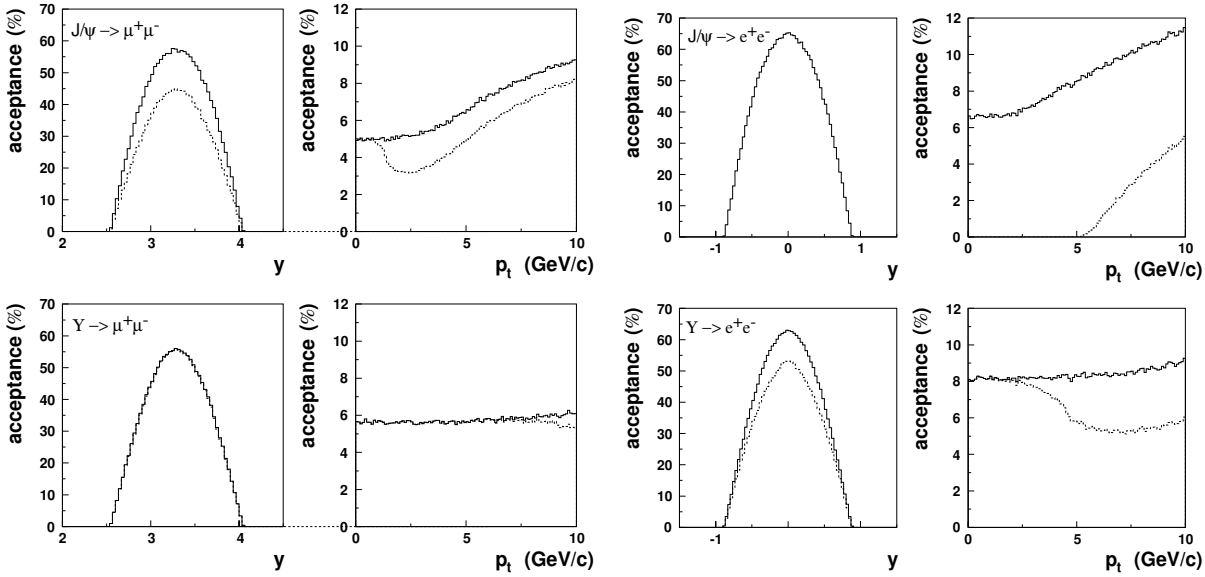


**Fig. 6:** Acceptance for J/$\psi$ and $\Upsilon$ as a function of $y$ and $p_T$ for measurements in the di-muon channel and di-electron channels. To give an idea of the effect of the trigger, the acceptances are shown without (solid) and with (dashed) a sharp cut on the transverse momentum of single muons of 1 GeV/$c$ (2 GeV/$c$) for J/$\psi$ ($\Upsilon$ ) and for single electrons of 3 GeV.

Table 1 shows the main quarkonia detection characteristics of the TRD and the Muon Spectrometer and the acceptances for J/$\psi$ and $\Upsilon$ as a function of $y$ and $p_T$ are shown in Fig. 6.

**Table 1:** Main characteristics of quarkonia detection with the TRD and the Muon Spectrometer in ALICE.

| | Muon Spectrometer | TRD |
|---|---|---|
| Acceptance | $2.5 < \eta < 4$ | $\|\eta\| < 0.9$ |
| Mass Resolution J/$\psi$ | 72 MeV | 34 MeV |
| Mass Resolution $\Upsilon$ | 99 MeV | 93 MeV |

In one year of pp running at $\langle L \rangle = 3 \times 10^{30}$ cm$^{-2}$s$^{-1}$ ALICE will detect several $10^6$ J/$\psi$s and several $10^4$ $\Upsilon$s in the di-muon channel. A $\Upsilon$ statistics of $10^2$–$10^3$ can be obtained in the di-electron channel. For the J/$\psi$ we expect $\approx 10^4$ untriggered low-$p_T$ and $\approx 10^4$ high-$p_T$ triggered events.

## References


[1] ALICE Collaboration, ALICE Technical Proposal, CERN/LHCC 95-71 (1995).

[2] ALICE Collaboration, ALICE Physics Performance Report,Vol. I, CERN/LHCC 2003-49 (2003).

[3] ATLAS Collaboration, ATLAS Technical Proposal, CERN/LHCC 94-43 (1994).

[4] CMS Collaboration, The Compact Muon Solenoid Technical Proposal, CERN/LHCC 94-38, LHCC/P1 (1994).

[5] LHCb Collaboration, LHCb Technical Proposal, CERN/LHCC 98-004 (1998).

[6] ATLAS Collaboration, High-Level Trigger, Data Acquisition and Controls TDR, CERN/LHCC 2003-022 (2003).

[7] J. Baines, for the ATLAS Collaboration, ATLAS B-trigger Update, Nucl. Phys. Proc. Suppl. 120 (2003) 139 (2003).

[8] CMS Collaboration, CMS: The Tracker Project Technical Design Report, CERN/LHCC 98-06, CMS TDR 5 (1998).

[9] CMS Collaboration, Addendum to the CMS Tracker TDR, CERN/LHCC 2000-016, CMS TDR 5 Addendum 1 (2000).

[10] CMS Collaboration, CMS: The Trigger and Data Acquisition Project, Volume I: The Level-1 Trigger TDR, CERN/LHCC 2000-038, CMS TDR 6.1 (2000).

[11] CMS Collaboration, CMS: The Trigger and Data Acquisition Project, Volume II: Data Acquisition and High-Level Trigger TDR, CERN/LHCC 2002-26, CMS TDR 6.2 (2002).

[12] LHCb Collaboration, LHCb Trigger TDR, CERN/LHCC 2003-031 (2003).

[13] LHCb Collaboration, LHCb Computing TDR, in preparation.

[14] N. Carrer and A. Dainese, ALICE Internal Note, ALICE-INT-2003-019 [arXiv:hep-ph/0311225] (2003).

[15] N. Carrer, A. Dainese and R. Turrisi, J. Phys. **G 29**, 575 (2003).

[16] A. Dainese, Ph.D. Thesis, Università degli Studi di Padova [arXiv:nucl-ex/0311004] (2003).

[17] ALICE Collaboration, ALICE Physics Performance Report, Vol. II, in preparation.

[18] M. Mangano, P. Nason and G. Ridolfi, Nucl. Phys. **B 373**, 295 (1998).

[19] ATLAS Collaboration, ATLAS Detector and Physics Performance Technical Design Report, CERN/LHCC 99-14 (1999).

[20] S. Robins, ATLAS Internal Note, ATL-PHYS-2000-026 (2000).

[21] Th. Lagouri, Eur. Phys. J. **C 33**, S497 (2004).

[22] Th. Lagouri, ATLAS Internal Note, ATL-COM-PHYS-2004-063 (2004).

[23] S.P. Baranov and M. Smizanska, Phys. Rev. **D 62**, 014012 (2000).

[24] H. Satz, Nucl. Phys. **A 590**, 63c (1995).

[25] T. Matsui and H. Satz, Phys. Lett. **B 178**, 416 (1995).

[26] D. Kharzeev and H. Satz, Phys. Lett. **B 334**, 155 (1994).